

AutoGate: Fast and Automatic Doppler Gate Localization in B-mode Echocardiogram

JinHyeong Park¹, S. Kevin Zhou¹, Costas Simopoulos², and Dorin Comaniciu¹

¹ Integrated Data Systems, Siemens Corporate Research, Inc., Princeton, NJ, USA
{jin-hyeong.park, shaohua.zhou, dorin.comaniciu}@siemens.com,

² Ultrasound Division, Siemens Medical Solution, Mountain View, CA, USA. *
costas.simopoulos@gmail.com,

Abstract. In this paper, we propose a so-called **AutoGate** algorithm for fast and automatic Doppler gate localization in B-mode echocardiography. The algorithm has two components: 1) cardiac standard view classification and 2) gate location inference. For cardiac view classification, we incorporate the probabilistic boosting network (PBN) principle to local-structure-dependent object classification, which speeds up the processing time as it breaks down the computational dependency on the number of classes. The gate location is computed using a data-driven shape inference approach. Online clinical evaluation was performed by integrating the algorithm to a real machine. Experiment results show that the proposed algorithm performs very comparable to expert manual gate placement. To the best of our knowledge, this is the first to provide a feasible solution to automate the Doppler gate placement in real time environment.

1 Introduction

The Doppler echocardiography is widely used to assess cardiovascular functionalities such as valvular regurgitation and stenosis. It is captured by a Doppler ultrasound transducer that employs the Doppler effect to determine whether structures (usually blood) are moving towards or away from the ultrasound probe, and its relative velocity [1]. To acquire a Doppler echocardiogram, a sonographer needs to manually locate a so-called Doppler gate on the top of a B-mode echocardiogram where the velocity and direction of blood are to be sampled by the Doppler transducer.

In this paper, we propose a fast and robust algorithm for automatic Doppler gate localization, which is called (**AutoGate**) afterward. **AutoGate** employs data-driven machine learning techniques customized for medical image analysis tasks such as left ventricle (LV) detection in noisy echo images using binary classification, multi-class classification, shape inference etc. The benefit of automatic placement of the Doppler gate can be summarized into two aspects:

* This author currently works for U-Systems Inc.

reducing the duration of imaging work flow and increasing the consistency of gate localization.

The proposed **AutoGate** algorithm has two main components: (i) fast cardiac view classifier and (ii) gate location inference model. To automate the gate localization, we should first identify the cardiac view of the B-mode because each standard cardiac view shows different valves where a gate is located to capture the Doppler signal. Once the view is determined using the view classifier, **AutoGate** invokes the inference model to estimate the final gate location. We base the inference model on the database-guided segmentation approach proposed in [2]. It is trained to build a function which computes the LV shape and the gate location using an image patch. Actually, we simultaneously infer the LV shape and the gate location using the shape inference algorithm [2].

There are some previous works to directly deal with automatic view classification of echocardiogram [3][4][5][6][7]. We propose a fast cardiac view classification algorithm based on the Local Structure Dependent Classification approach (called *fLoDeC*) by adopting the basic algorithm of *CardiacVC* proposed in [3] and Probabilistic Boosting Network (PBN) framework proposed in [8]. Due to the use of PBN, *fLoDeC* is more scalable than *CardiacVC*. In other words, the computation time is affected less for *fLoDeC* than for *CardiacVC* as the number of object classes increases.

We performed experiments for four cardiac standard views: apical four chamber (A4C) view, apical two chamber (A2C) view, apical three chamber (A3C) view, and apical five chamber (A5C) view. A gate is located on mitral valve (MV), tricuspid valve (TV), or aortic valve (AV) depending on the view type.

2 Object Detection and Classification

In this section we propose a generic algorithm of fast object detection and classification called *fLoDeC*. The basic framework of this algorithm is to anchor a relatively stable (rigid) local structure of each object class. We use the LV as the local structure. A global structure is then extracted based on the anchored local structure and further classified using multi-class classifiers. *fLoDeC* uses the same idea of local-structure-dependent detection and classification from *CardiacCV* [3], but it incorporates the PBN principle [8] to achieve further speed-up. The diagram in Fig. 1 illustrates how *fLoDeC* is constructed using the PBN framework.

Based on the diagram in Fig. 1-(a), the *fLoDeC* algorithm is summarized as follows. Each local structure detector (LSD_i), where $i \in [1, C]$, is independently applied to an echocardiogram. The LSD_i provides positive candidates of the local structure of the i^{th} object class. The training data for the global structure classifiers are constructed based on these positive candidates by applying LSD_i to not only the images of the i^{th} object class but also those of the other classes. Therefore, the global structure training data set is local-structure-dependent, based on which we learn a multiclass global structure classifier ($MGSC_i$). The final classification result is computed by integrating the classification results provided by $\{MGSC_1, \dots, MGSC_C\}$.

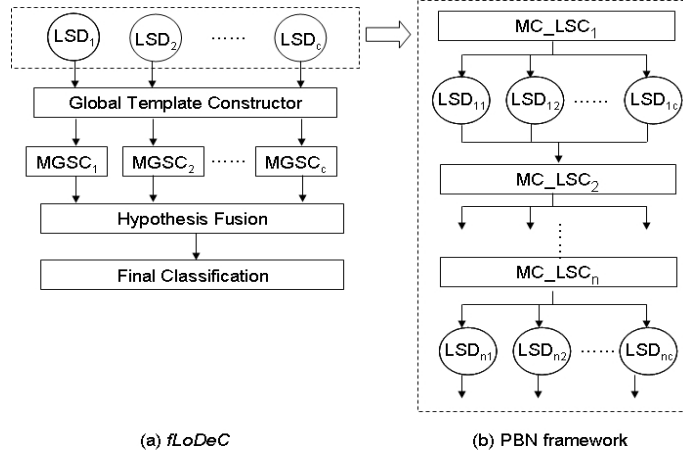


Fig. 1. Multiple object detection and classification using local structure dependent classification approach. **LSD**: Local Structure Detector, **LSC**: Local Structure classifier, **MGSC**: Multi-class Global Structure Classifier.

To anchor the local structures, all the *LSD*'s should exhaustively search the image to detect their own local structures. The search space for LV is of five dimensions: (x, y) location, width, height and angle, represented as (x, y, w, h, θ) . This is the most time consuming part of *fLoDeC* because each local structure detector should be applied in the five dimensional search space independently. The computation time linearly depends on the number of object classes.

To break down the above linear computational dependency on the number of classes, the *fLoDeC* algorithm tackles the problem by replacing the local structure detection part, inside the dashed box in Fig. 1-(a), with the PBN structure shown in Fig. 1-(b). In this framework, we train one multi-class local structure classifier (*MC_LSC*), and configure it to multiple levels in a hierarchical structure, $MC_LSC_1, \dots, MC_LSC_n$. To classify a local structure, it should be supplied from MC_LSC_1 to MC_LSC_n sequentially. Each local detector, LSD_i , is also re-configured as a hierarchical structure by decomposing it into multiple levels of weak detectors in the same manner of *MC_LSC*. The decomposed $MC_LSC_1, \dots, MC_LSC_n$ and $LSD_{1i}, \dots, LSD_{ni}$ are grouped in a graph structure shown in Fig. 1-(b). The essence of this approach can be summarized into two aspects: 1) apply only the few selected local structure detectors based on the *MC_LSC*, and 2) the graph structure further enables the negative exclusion as soon as possible from early layers.

The final view classification result, \hat{c} , given a candidate image I , can be computed via the MAP rule:

$$\hat{c} = \arg \min_{i \in [1, C]} \{P(c_i|I) = \sum_{j=1}^C P_{MGSC}(c_i|j, I) P_{LSD}(j|I)\}, \quad (1)$$

where $P_{MGSC}(c_i|j, I)$ is the posterior probability of being class c_i from $MGSC_j$ and $P_{LSD}(j|I)$ is the prior probability from LSD_j .

2.1 Cardiac View Classification of Four Apical Views

We will discuss about how the cardiac view classifier in **AutoGate** is implemented using *fLoDeC* presented in Sec. 2. We focus on the echocardiograms of four apical views, namely A4C, A2C, A3C and A5C.

To construct *fLoDeC* to deal with the four views, we train one LV classifier (*MC.LSC*), four LV detectors, LSD_{A4C} , LSD_{A2C} , LSD_{A3C} and LSD_{A5C} , as local structure detectors, and four global view classifiers, $MGSC_{A4C}$, $MGSC_{A2C}$, $MGSC_{A3C}$ and $MGSC_{A5C}$. Each local structure detector is trained based on Probabilistic Boosting Tree (PBT) [9] which treats this detection problem as a two-class classification problem (positive class versus negative class). The LV-classifier and the four cardiac view classifiers are trained using the multi-class logit boosting based image classification approach [3][10]. The weak classifiers in (*MC.LSC*) and *LSD*'s are divided into several parts to form the PBN framework shown in Fig. 1-(b).

3 Automatic Gate Localization Based on Learning-based Approach

Once the view is determined, we need to find the best location of the Doppler gate. It is, however, a hard problem because the gate is usually located on the path of blood flow which is an open space. To tackle this, we utilize anatomy structure such as LV and valves around the gate location to infer the target gate location. The LV shape and its corresponding gate locations are annotated by experts using points (17 points for LV and one point for each gate) as shown in 2. In this figure, the yellow dots represent an LV shape and the red circles with a dot represent gate locations. In A4C view, two gate locations are computed: one for mitral valve and the other for tricuspid valve. Only one Doppler gate of mitral valve is computed in A2C view. Two gate locations, one for mitral valve and aortic valve, are annotated in A3C view and A5C view.

With these annotations, the gate locations, even though it is ambiguous itself, can be inferred using the other heart anatomy structure such as LV, aortic valve annulus, tricuspid valve annulus, and so on.

We employ the database-guided segmentation algorithm proposed in [2] to infer LV shape and gate location simultaneously. The algorithm is summarized as follows. Each training image is represented using a very high dimensional numerical feature vector, and its shape (including both the LV shape and gate locations) is represented as a set of landmark points. The training data are clustered into several clusters in the shape space. The algorithm selects a small number of useful features based on boosting framework by maximizing the Fisher separation criterion of the clusters.

If the view is determined as \hat{c} , the LV image patch computed by $LSD_{\hat{c}}$ is used as an input for the shape inference model to locate the Doppler gate. The LV shape and the image appearance around the LV collaboratively contribute to the final gate locations.

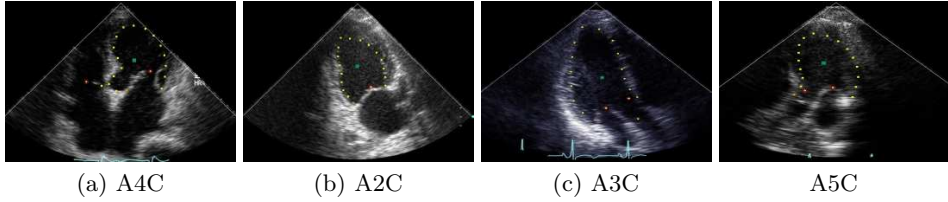


Fig. 2. Annotation of LV shape (yellow dots) and gate location (red circle with yellow dot inside).

4 Performance Evaluation

4.1 Offline Clinical Evaluation

For offline evaluation, we collected training data and test data separately. **AutoGate** was built using the training data and compute the classification accuracy and gate localization using both data sets. Table 1 shows two confusion matrix of the classification accuracy for training and test data which are very diverse in terms of not only image quality but also hear conditions. The average classification accuracy of training data is over 96%, and that of test data is close to 95%. As shown in Table 1, most of the classification error comes from the misclassification of A5C to A4C. It is because some A5C views have very small aorta structure which makes it very similar to A4C view.

Table 2 shows the distance of the gate location between **AutoGate** and expert’s annotation. As shown in the table, **AutoGate** localizes the gate location very comparable to experts.

Training Data (%)					Test Data (%)				
	A4C	A2C	A3C	A5C		A4C	A2C	A3C	A5C
A4C(408)	97.5	0.2	0.5	1.7	A4C(23)	100.0	0.0	0.0	0.0
A2C(296)	0.3	99.7	0.0	0.0	A2C(24)	0.0	96.0	4.0	0.0
A3C(410)	1.0	3.7	94.6	0.7	A3C(25)	0.0	8.0	96.4	0
A5C(200)	8.0	0.0	0.0	92.0	A5C(24)	13.0	0.0	4.0	83.0

Table 1. Confusion matrix of view classification results. The numbers in a parenthesis represents the number of training/test data

Fig. 3 shows the valve localization results by applying the offline version of the **AutoGate** algorithm to dicom videos. The small two horizontal lines within the pan box indicate the gate location. In this figure, ED and ES stand for End of Diastole and End of Systole, respectively. The view classification result is illustrated using blue bars along with probabilities of being A4C, A2C, A3C and A5C (from left to right) below each picture.

4.2 Online Clinical Evaluation

For online evaluation, we integrated the online version of **AutoGate** algorithm into a real ACUSON *sequoiaTM* ultrasound machine, and computed the actual

	Mitral Valve		Tricuspid Valve		Aortic Valve	
	Mean (mm)	Std (mm)	Mean (mm)	Std (mm)	Mean (mm)	Std (mm)
A4C	4.2	2.5	3.4	2.5	-	-
A2C	5.9	2.4	-	-	-	-
A3C	3.5	2.2	-	-	3.4	2.3
A5C	3.6	3.6	-	-	2.4	2.4

Table 2. Gate localization error between **AutoGate** and an expert for test data. ”-” indicates ”Not Applicable”.

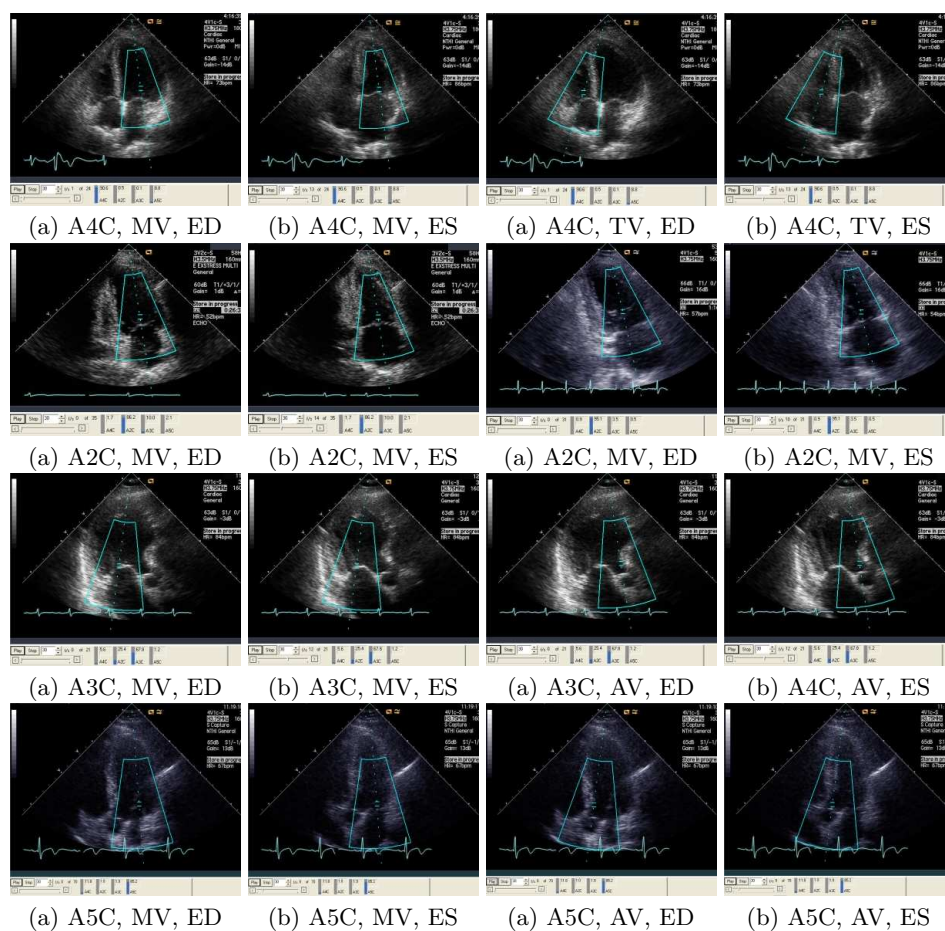


Fig. 3. Valve localization results in offline environment. MV and TV represent Mitral Valve and Tricuspid Valve, respectively. ED and ES stand for End diastole and End Systole, respectively.

Doppler measurements from the Doppler signal captured after locating the gate using **AutoGate**. This measurements are compared with those computed after manually placing the gate by experts. The whole **AutoGate** algorithm runs within one second on the ultrasound machine.

Fig. 4 illustrates two scatter plots of MV peak velocity measures. In this Figure, the left scatter plot shows peak velocities computed by placing a gate using **AutoGate** (x-axis) and mean peak velocities computed after placing a gate twice by a expert (y-axis). The right scatter plot shows intra-user variability. As shown in the scatter plots, the correlation coefficient between **AutoGate** versus the expert is 0.951 which is very comparable with intra-expert variability, 0.966. It is also reported by the evaluator that the gate placement by **AutoGate** was appropriate 100% of the time. Minor adjustments were done 30% of the time but with no significant effect on spectral Doppler strip.

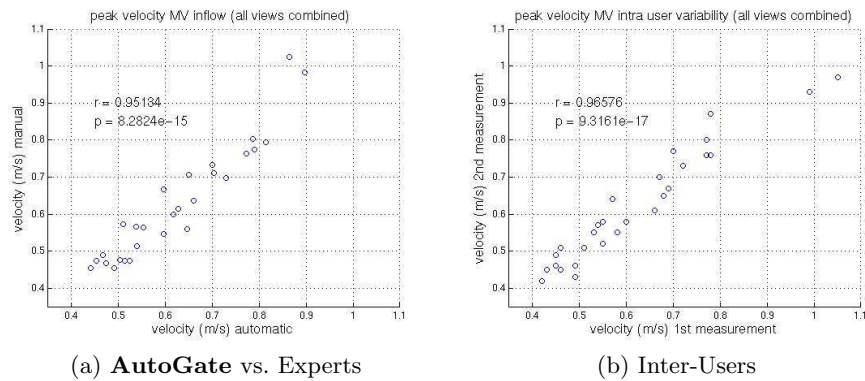


Fig. 4. Correlation coefficient of MV inflow peak velocity

Fig. 5 shows Doppler echocardiogram of Left Ventricular Outflow Tract (LVOT) by **AutoGate** in (a) and by expert in (b), and that of Mitral valve inflow by **AutoGate** in (c) and by expert in (d). They look strikingly similar.

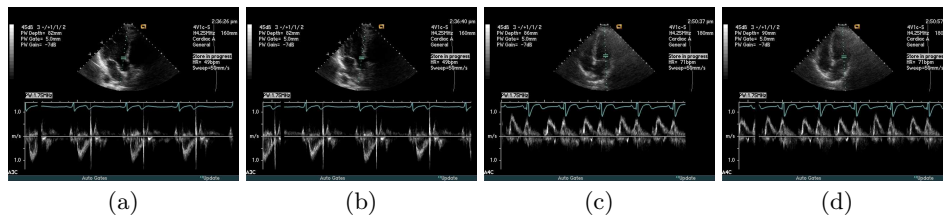


Fig. 5. Spectral Doppler signal captured after placing Doppler gate by **AutoGate** or an expert. (a) LVOT signal from **AutoGate**, (b) LVOT signal from Expert, (c) MV Inflow signal by **AutoGate**, (d) Mitral Valve Inflow signal by Expert

5 Conclusion

We proposed a fast algorithm of automatic Doppler gate localization, **AutoGate**, in B-mode echocardiogram. To improve the scalability, we developed a faster version of local-structure-dependent classification algorithm *fLoDeC*, which breaks down the linear dependency on the number of object classes, by employing the Probabilistic Boosting Network (**PBN**) principle. *fLoDeC* anchors the LV structure and classifies the cardiac view faster than *CardiacAC*[3], which is the most time consuming part of AutoGate algorithm. The final gate location is computed by utilizing the explicit heart anatomy structure such as Left Ventricle (LV) and valve planes.

In term of performance, **AutoGate** performs very comparable to the manual gate localization by expert, and is expected to reduce the duration of imaging work flow for spectral Doppler analysis. To the best of our knowledge, this is the first attempt to provide a feasible solution to automate the gate placement in real time environment.

References

1. Feigenbaum, H., W., A., Ryan, T.: Feigebaum's Echocardiography. Lippincott Williams & Wilkins (2005)
2. Georgescu, B., Zhou, X.S., Comaniciu, D., Gupta, A.: Database-guided segmentation of anatomical structures with complex appearance. In: CVPR. (2005) 429–436
3. Park, J., Zhou, S., , Georgescu, B., Simopoulos, J., Otsuki, J., Comaniciu, D.: Automatic cardiac view classification of echocardiogram. In: iccv. (2007)
4. Aschkenasy, S.V., Jansen, C., Osterwalder, R., Linka, A., Unser, M., Marsch, S., Hunziker, P.: Unsupervised image classification of medical ultrasound data by multiresolution elastic registration. *Ultrasound in Medicine and Biology* **32**(7) (2006) 1047–1054
5. Zhou, S.K., Park, J., Georgescu, B., Simopoulos, J., Otsuki, J., Comaniciu, D.: Image-based multiclass boosting and echocardiographic view classification. In: CVPR. (2006) 1559– 1565
6. Otey, M., Bi, J., Krishna, S., Rao, B., Stoeckel, J., Katz, A.S., Han, J., Parthasarathy, S.: Automatic view recognition for cardiac ultrasound images. In: in Proceedings of Int'l Workshop on Computer Vision for Intravascular and Intracardiac Imaging. (2006) 187–194
7. Ebadollahi, S., Chang, S.F., Wu, H.: Automatic view recognition in echocardiogram videos using parts-based representation. In: CVPR. Volume II. (2004) 2–9
8. Zhang, J., Zhou, S., Comaniciu, D.: Joint real-time object detection and pose estimation using probabilistic boosting network. In: cvpr. (2007)
9. Tu, Z.: Probabilistic boosting-tree: Learning discriminative models for classification, recognition, and clustering. In: ICCV. (2005) 1589– 1596
10. Friedman, J., Hastie, T., Tibshirani, R.: Additive logistic regression: a statistical view of boosting. *Ann. Statist.* **28**(2) (2000) 337–407